Volumetric and Phase Behavior of Acetonitrile at Temperatures from 363 to 463 K

Witold Warowny

Institute of Physical Chemistry, Polish Academy of Sciences, ul. Kasprzaka 44/52, 01-224 Warszawa, Poland

An apparatus to perform volumetric measurements of fluid-phase pure compounds and binary mixtures has been tested by the measurements of 11 vapor pressures and 18 saturated densities of acetonitrile, at intervals of 10 K, over the temperature range 363.15–463.15 K. For the gas phase, density and virial coefficients corrected for adsorption were determined, without knowing the compound's volume or mass, over the temperature range from 403.15 to 463.15 K.

Introduction

There has been increasing interest in the volumetric and phase behavior of systems, particularly those containing hydrocarbons and a polar component, which is frequently used as a solvent. Acetonitrile serves as an excellent solvent for many polar or ionized organic compounds. Saturated hydrocarbons are insoluble. The work reported in this paper represents part of a continuing study on the properties and phase behavior of binary systems containing acetonitrile and light hydrocarbons. Information on binary systems is required for evaluating the parameters used for predicting the behavior of multicomponent systems. Limited literature data on the vapor pressure, saturated and gas densities, and virial coefficients of acetonitrile, a compression/decompression procedure involving adsorption phenomena, and testing of the apparatus were the other purposes motivating the present investigation.

Possibilities of measuring various kinds of fluid equilibria, including critical points and three fluid phases for binary mixtures, were decisive in selecting the static visual method. A certain advantage of this method is the results obtained along the coexistence curve, which are preferred for theoretical interpretation.

Experimental Section

Materials. Fluka's UV spectroscopy grade acetonitrile with purity guaranteed to be greater than 99.5% was used. Possible impurities included water, unsaturated nitriles, acetamide, ammonium acetate, acetic acid, aldehydes, amines, and ammonia. The acetonitrile was further purified by contacting activated molecular sieves to adsorb traces of moisture and degassed by several cycles of freezing and melting carried out under dynamic vacuum conditions. Degassing is crucial for vapor-pressure measurements to be accurate.

Apparatus. The method was earlier used in this laboratory by Kreglewski and Zawisza (*1*, *2*). A new arrangement of the experimental apparatus used in this work is shown schematically in Figure 1. This operates over the temperature range 280–480 K and at pressures ranging from subatmospheric up to the limit of strength of a glass tube, 8 MPa, at room temperature.

The heart of the apparatus is a precision bore glass tube, 1, immersed in a silicone oil bath, 2. The upper end of the tube was welded; the lower end, outside the oil bath, was restricted by a valve, 3. A Viton O-ring was compressed to seal valve 3 to the flattened and polished end of the tube. The tube consisted of two parts: the upper one 50 mm long, 3.28-mm i.d., and the lower part, with valve 3 at the end, 400 mm long, 8.29-mm i.d., and having a length of 300 mm immersed in the bath. The maximum working volume was approximately 15 cm^3. The fluid under study was confined by mercury. The mercury-press screw pump displaced mercury inside the tube and was connected with a mercury differential pressure indicator. The mercury pump was connected to a mercury reservoir filled with high-purity distilled mercury under vacuum. A diode sensor indicated the level of mercury.

Three mechanical vacuum pumps and a mercury diffusion pump with cold traps were used to evacuate various portions of the system to about 0.001 Pa.

Measurement Systems. The pressure of the fluid was transmitted by mercury to the mercury differential pressure indicator. The other side of the diaphragm was balanced by nitrogen. The pressure was read by an air dead weight gauge or by an oil dead weight gauge (via an oil differential pressure indicator). The air dead weight gauge (Ruska Instrument Corp., model 2465-754) had two overlapping ranges, 1.4–172 and 14–7000 kPa, with a stated accuracy of better than ±0.01% of the full range. After recalibration of the oil dead weight gauge, the original accuracy, ±0.03%, was improved to become ±0.02%.

Pressure corrections were made for the gravitational effect, distortion of the effective piston area due to pressure and temperature changes, buoyancy of air, and hydrostatic columns of mercury, oil, and air.

Two null transducers with digital monitors served as the pressure-sensing element. They were equipped with 0.04-mm-thick stainless steel diaphragms. The mercury inside the mercury differential pressure indicator and the oil inside the oil differential pressure indicator contacted the bottom part of the diaphragms. Nitrogen gas balanced the upper part of the diaphragms in the two differential pressure indicators. Deflection of the diaphragm was transferred to the core of the differential transformer coil. The null position must be calibrated periodically, and this is a major disadvantage. Both transducers have a null readout with a sensitivity of 2 Pa.

Prior to any analysis of the results, the measured pressures were corrected for the deviations of the measured temperature from the exact isotherm. The saturated vapor pressure of mercury was subtracted from a measured pressure. The main sources of the cumulated uncertainties were the hydrostatic pressure of mercury, the saturated vapor pressure of mercury, and the correction of the differential pressure indicators for the null setting shifting with pressure and time. An accuracy of ±0.05% was associated with the pressure measurement system.

0021-9568/94/1739-0275$04.50/0

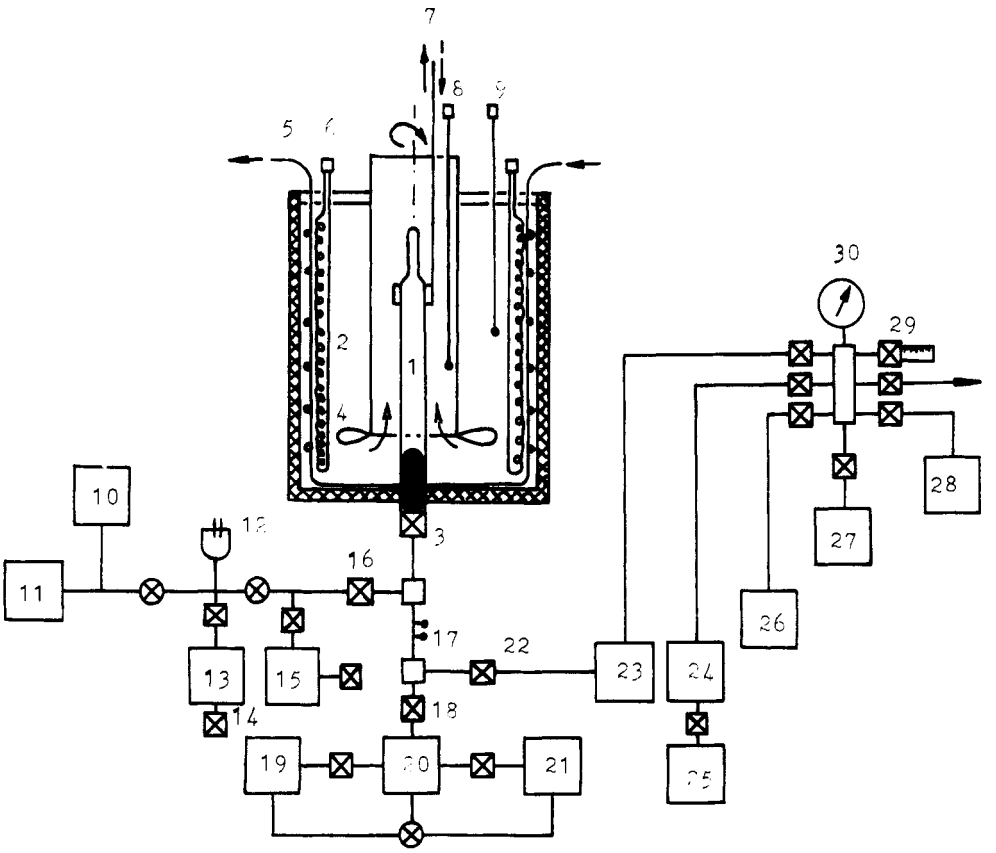

Figure 1. A simplified schematic diagram of the experimental apparatus: (1) glass tube; (2) silicone oil bath; (3) special needle valve; (4) stirrer, (5) cooling coil; (6) heater; (7) permanent magnet; (8) platinum resistance thermometer; (9) sensor; (10) main vacuum system; (11) glass filling system; (12) thermocouple; (13) crusher; (15) glass–metallic charging system; (17) diode sensor; (19) vacuum system; (20) mercury press screw pump; (21) mercury reservoir; (23 and 24) diaphragm zero pressure indicators; (25) Budenberg oil dead weight gauge; (26) Ruska air dead weight gauge; (27); air pump (28) nitrogen storage vessel; (29) micrometer needle valve; (30) Heise gauge; (⊗) vacuum valves; (⊠) high-pressure valves.

The double-wall thermostat divided into two chambers was movable along rails. The outer chamber was furnished with a cooling coil and two heaters. One heater (40 W) was controlled by a sensor of the proportional-integrating regulator. The inner rotating chamber, equipped with a stirrer, had vertical holes in order to read the mercury levels inside the measuring tube.

The temperature measuring system consisted of a type G-2 Mueller bridge (Leeds and Northrup Co.), a platinum resistance thermometer, and a galvanometer used as a null detector. The temperature in the inner chamber was measured with a Tinsley platinum resistance thermometer (no. 217967), calibrated at the NPL, Teddington, England, on the IPTS-68. For monitoring the temperature, a digital Hewlett-Packard quartz thermometer was used. Near the glass tube, temperature was uniform and constant to within ±2 mK, and it was measured with a maximum uncertainty of ±5 mK.

The volume of the tube at any height from the sealed end was calibrated with mercury. The levels of mercury were measured by a cathetometer precise to within ±0.01 mm. The volume of the tube was determined with an overall accuracy of ±0.1% at 293.15 K. The diameter of the tube was ±0.005 cm. Appropriate volume corrections were made for the thermal expansion of Pyrex glass and for the variation of the internal radius with pressure. The pressure distortion coefficient, as calculated from the theory of elasticity, is

$$\xi_i = 1 + 4.94 \times 10^{-8}(p_i/\text{kPa}) \qquad (1)$$

Two separate filling systems were designed. The first one, a glass system, was for substances boiling above room temperature. For more volatile substances a glass–metallic system was used. Known masses of degassed samples were prepared in glass capillary ampules placed in a crusher. The end of the tube valve was kept frozen by liquid nitrogen to transfer the whole amount of the substance from the crusher.

Measurement Procedure. Measurements were made by observing the pressure and the corresponding level of mercury after several isothermal compressions or decompressions of a known amount of the substance inside the calibrated glass tube. Mercury was used as a medium for pressure and volume measurements. Stirring of the sample was accomplished with the aid of a steel ball 0.15 cm in diameter, which was moved along the tube by an external permanent magnet.

At the beginning, the gas inside the tube was under some reference pressure p_r and the corresponding mercury level H_r. The reference pressure in the gas phase was arbitrary. The decompression or compression process below or above an arbitrary level H_r was performed a sufficient number of times to establish the sequence of pressures. Subscripts i are between subscripts 1 and n, and $1 \le r \le n$. This part of the isotherm was used to calculate gas densities and virial coefficients.

After the gas was compressed, temperature and pressure was taken at the moment of the transition of the single-phase system into the two-phase system, i.e., at the appearance of the first drop of the liquid corresponding to the dew point. With the 8.29-mm-i.d. tube, visual determination of the exact mercury level at which the last liquid drop disappears was difficult. The dew point was confirmed by intersection of the two curves describing the $p-V$ isothermal slopes in this region.

The volume was diminished by displacing the mercury, and when the last bubble of vapor disappeared or just before the first bubble of vapor appeared, pressure and temperature were measured. The bubble point pressure and volume were measured in the thick part of the glass tube.

Analysis of the Gas Phase. Usually the second and third virial coefficients B and C are evaluated from experimental quantities p, T, and $\rho = n/V$, by utilizing the following equation:

$$Z = p/(\rho RT) = 1 + B\rho + C\rho^2 + ... \quad (2)$$

where Z is the compression factor, R is the gas constant, p is pressure, T is temperature, ρ is density, n is the amount of the gas, and V is the volume of the system. The molar mass of acetonitrile is 41.05 g mol^{-1} (3). Since accurate volume values are difficult to measure, a cross-checking method called the compression/decompression (c/d) procedure was developed. This method does not require a direct measurement of the volume or mass.

At an arbitrary reference point (subscript r), the equation of state is

$$\rho_r = p_r/(Z_r RT) = n_r/V_r' \quad (3)$$

When the adsorption occurs on the tube–mercury surfaces, the law of mass conservation no longer holds true, and then, at an ith pressure, relationship 3 becomes

$$\rho_i = p_i/(Z_i RT) = n_i/V_i' = (n_r + m_r - m_i)/V_i' \quad (4)$$

$$V_i' = V_i\xi_i = [V_r + S(H_r - H_i)]\xi_i \quad (5)$$

where n_r, the amount of free gas, corresponds to an exerted pressure p_r, m_r, is the amount of the gas adsorbed on the surface in a volume V_r', m_i represents the amount of the gas adsorbed in a volume V_i' under pressure p_i, V_r and V_i are the volumes referred to zero pressure, and H_i is the corresponding mercury level inside the tube; subscript i denotes the number in the sequence of p, V, H, etc. In the measured range of heights, the inner diameter of the tube must be constant. The ratio of the area of the tube cross-section S to volume V_r is denoted by K_r and is called the isothermal tube constant at zero pressure. Division of eq 4 by eq 3 produces

$$\rho_i = (\xi_r/\xi_i)(\rho_r + \rho_r^{ads})/\{1 + K_r(H_r - H_i)\} - \rho_i^{ads} \quad (6)$$

$$\rho_i^{ads} = m_i/V_i' = k_A p_i^R/\{(1 - p_i^R)(1 + k_B p_i^R)\} \quad (7)$$

$$p_i^R = p_i/p^s \quad (8)$$

The density defined by the left part of eq 7 is termed the adsorption bulk density. This is the ratio of the amount of the gas adsorbed on the glass and mercury surfaces to the volume of free gas. Equation 7 employs an arbitrary adsorption model; to choose a correct model is both necessary and sufficient. Here the Brunauer–Emmett–Teller (BET) adsorption model was used, where k_A and k_B are adsorption constants, and p^s is the vapor pressure.

If adsorption does not occur, $n_r = n_i$, the last term in eq 6 vanishes ($\rho_r^{ads} = 0$ and $\rho_i^{ads} = 0$).

Experimental pressures on the isotherm are independent of each other and can be removed without any consequence for further calculations. The objective function for a nonlinear least-squares analysis is

$$F = \sum_i W_i[p_i/(RT) - \sum_{s=1}^{3} A_s(\rho_i)^s]^2 = \text{minimum} \quad (9)$$

Table 1. Vapor Pressure and Saturated Molar Densities of Acetonitrile

		ρ^v/(mol m^{-3})			ρ^L/(mol m^{-3})		
T/K	p^s/kPa this work	this work	ref 6	ref 7	this work	ref 5	ref 6
363.15	130.42				17 181		
373.15	173.96				16 914		
373.15							17 028
376.69						16 727	
383.15	229.48				16 614		
393.15	297.88				16 294		
403.15	378.52	138.37			15 966		
413.15	478.11	191.96			15 627		
422.69						15 258	
423.15	592.23	238.25			15 298		
423.15			240.7				15 469
433.15	729.42	290.38			14 942		
438.9				329.24			
442.6				357.77			
443.15	887.64	352.01			14 614		
444.12						14 486	
444.5				364.13			
453.15	1081.09	428.50			14 207		
455.7				469.92			
456.62						14 000	
460.2				524.90			
463.15	1305.73	494.77			13 816		

W is the weighting factor, and A_s are virial coefficients; $A_1 = 1$, $A_2 = B$, and $A_3 = C$. The Hall–Canfield criterion (4) provides a method for choosing an optimal number of virial coefficients. For the purposes of this paper, the value of K_r was found by earlier calibration of the tube. Minimization of eq 9 produces the reference gas density ρ_r, $s - 1$ virial coefficients, and u adsorption constants. Here $u = 2$, viz., k_A and k_B.

In general, K_r can be treated as an independent parameter during the minimization of the objective function (9).

Results and Discussion

Vapor Pressure. Performance of the apparatus was evaluated by measuring vapor pressures of acetonitrile at 10 K intervals over the temperature range 363.15–463.15 K. This was an excellent test for the compound's purity and for ascertaining the best operating conditions.

Only three previous researchers (5–7) have covered the present range of measurements; for results of this work see Table 1. The present dew and bubble pressures oscillate to within 1–3 kPa as a result of 1000-fold compression of the volatile impurities (like remaining air) from the maximum volume to the bubble point volume. The vapor pressures of the bubble point are reported over the temperature range of 360–413 K; they are not corrected for compression of the impurities. At higher temperatures ranging from 423 to 463 K, dew points are presented which appear to be more reliable. The uncertainty was estimated to be ±0.05% for the dew point measurements. The combined values of the dew and bubble points of the present work were fitted to the Antoine- and to the Wagner et al.-type equations (8):

$$\ln(p^s/\text{kPa}) = a_A + b_A/(T/\text{K} + c_A) \quad (10)$$

$$\ln(p^s/p_c) = (T_c/T)(a_W\tau + b_W\tau^{1.5} + c_W\tau^{2.5} + d_W\tau^3) \quad (11)$$

where p^s is the vapor pressure, p_c is the critical pressure, and $\tau = (1 - T/T_c)$. The critical temperature and pressure were selected to be $T_c = 547.85$ K and $p_c = 4833.2$ kPa (3). The best values for the parameters were found to be $a_A = 15.020\,56$, $b_A = -3471.08$, $c_A = -21.123\,23$, $a_W = -5.035\,172$, $b_W = -9.644\,056$, $c_W = 46.857\,00$, and $d_W = -49.653\,03$. In Figures 2 and 3, the relative pressure deviations from the vapor

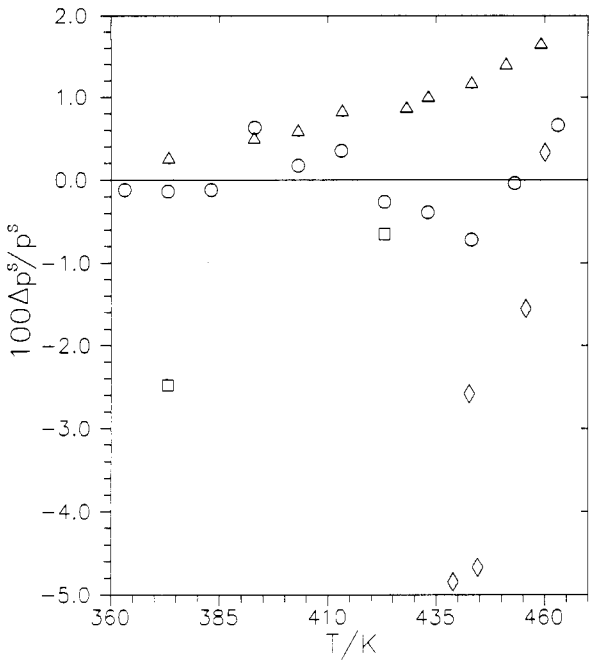

Figure 2. Fractional deviations $\Delta p^s/p^s = \{p^s - p^s(\text{calcd})\}/p^s$ of experimental vapor pressures from eq 10: ○, this work; △, ref 5; □, ref 6; ◇, ref 7.

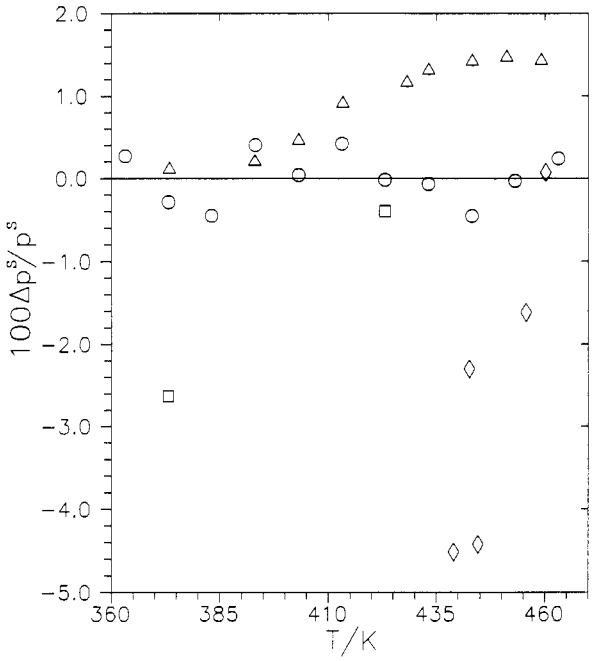

Figure 3. Fractional deviations $\Delta p^s/p^s = \{p^s - p^s(\text{calcd})\}/p^s$ of experimental vapor pressures from eq 11: ○, this work; △, ref 5; □, ref 6; ◇, ref 7.

pressure equations (10 and 11) are plotted for each experimental point as a function of temperature over the entire range. The present results are closest to those of Kratzke and Muller (*5*), which vary from eqs 10 and 11 to within 1.5%; the differences from the results of Francesconi et al. (*6*) and Mousa (*7*) are higher, 2.5% and 5%, respectively.

Saturated Densities. Columns 3–8 of Table 1 compare the experimental saturated vapor and saturated liquid densities with the literature data. In the temperature range of this table, scarce data of saturated densities are known (*5–7*). The uncertainties were estimated to be ±0.05% for the vapor saturated density and ±0.1% for the liquid saturated density. The experimental saturated liquid densities of this work were adjusted by a least-squares procedure to the

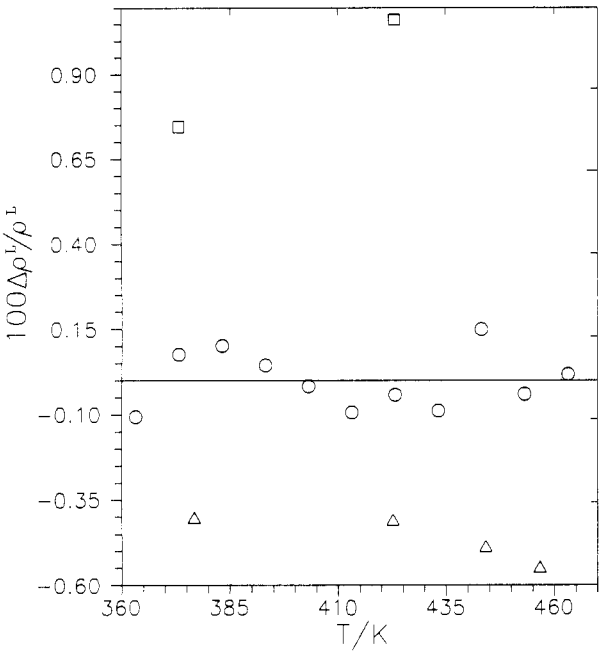

Figure 4. Relative density deviations $\Delta\rho^L/\rho^L = \{\rho^L - \rho^L(\text{calcd})\}/\rho^L$ of measured saturated liquid densities from eq 12: ○, this work; △, ref 5; □, ref 6.

Penterman–Wagner (*9*) equation

$$\rho^{LC} = 1 + a_{PW}\tau^{1/3} + b_{PW}\tau^{2/3} + c_{PW}\tau^3 \qquad (12)$$

where $\rho^{LC} = \rho^L/\rho_c$, ρ_c is the critical density, and ρ^L is the saturated liquid density. The critical density was selected to be $\rho_c = 5775.88$ mol m^{-3} (*10*). The coefficients of eq 12 are $a_{PW} = 1.850\,128$, $b_{PW} = 1.374\,607$, and $c_{PW} = 0.628\,563\,8$. The relative percentage deviation for the saturated density between the data of Table 1 and the results of eq 12 are presented in Figure 4. The present saturated liquid densities are seen to be between the data of refs 5 and 6. A small systematic shift of the relative deviation (0.5%) to the data of Kreatzke and Mueller (*5*) is observed.

Gas Phase. Measurements were performed on five isotherms at pressure intervals of 20–40 kPa. The lowest pressures were 120–130 kPa. Two independent pressure sets at temperatures of 423 and 443 K were measured. In order to check the reproducibility of the experimental points, some measurements were repeated.

The data on gaseous acetonitrile were reduced by using eq 9 and a least-squares minimization algorithm. Adsorption was expected to occur in these measurements because the maximum temperature of 463 K is well below the critical temperature of 548 K. Densities and virial coefficients were corrected for adsorption by the c/d procedure. Each experimental observation was given an equal weight.

The second virial coefficients of the acetonitrile were determined by a few researchers (*11–16*) over the reduced temperature range from 0.56 to 0.77 and above the critical temperature at 573.15, 623.15, and 673.15 K by Francesconi et al. (*6*). A significant scatter is observed, and the percentage deviations are within 5% in most cases and within 15% for the greatest difference. The present experimental values of the second virial coefficients and all the literature data are presented in Figure 5; the numerical data over the present experimental temperature range are listed in Table 2; over the temperature range 433.15–463.15 K virial coefficients have not yet been measured. The second virial coefficients agree well to within 0.5% at 423.15 K with the value of Kolysko et al. (*11*), and to within 3.5% at 403.15 K with the average value of the three measurements given by Lambert et al. (*16*).

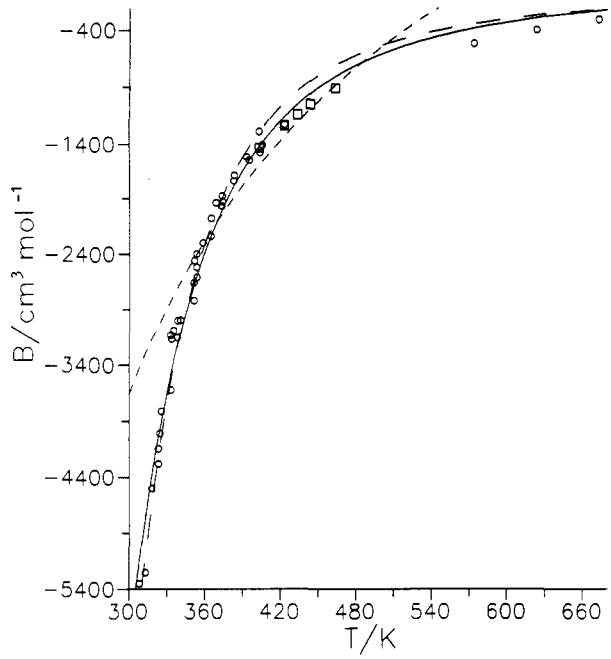

Figure 5. Experimental and correlated second virial coefficients: O, results of refs 6 and 11–16; □, this work; solid line, Tsonopoulos correlation; short dashed line, O'Connell and Prausnitz correlation; long dashed line, Tarakad and Danner correlation.

Table 2. Experimental Virial Coefficients for Acetonitrile

	$-B/(cm^3\ mol^{-1})$			$C \times 10^{-5}/(cm^6\ mol^{-2})$
T/K	this work	ref 11	ref 16	this work
403.15	1443.6			11.05
403.2		1290.0 ± 2		
404.2			1480	
405.4			1480	
405.6			1410	
423.15	1243.3			9.99
	1238.8			10.17
423.2		1230.0 ± 1		
433.15	1155.8			9.36
443.15	1070.9			6.53
	1075.2			8.10
463.15	940.4			4.42

The second virial coefficients at 403 K reported by Kolysko et al. (*11*) deviate significantly from the result (ca. 10%) of this work and (ca. 13.5%) of Lambert et al. (*16*). The present values are preferred, first because the volume was not measured, second because the precision of the temperature measurements was higher and the accuracy of the pressure measurement was comparable, third because some correction was made for adsorption, and finally because the third virial coefficient is included. Besides the experimental and adsorption uncertainties, the influence of the third and higher virial coefficients in the determination of the second virial coefficient from (p, ρ, T) data (when the virial equation of state (2) is truncated at the first order in ρ) has to be considered. The accuracy of the present second virial coefficient was estimated to be ±0.5%.

The original experimental data at 423.15 K (one from seven isothermal sets) and the results of calculations by the c/d procedure are presented in Table 3. This isotherm was measured twice, first by decompression of the fluid and next by compression to the starting point. If $r = n$, adsorption errors are minimized optimally. Adsorption causes more negative values of the second virial coefficients and higher density values when eq 9 is used to include the adsorption effect. Interpolated density data of the remaining sets were corrected for adsorption (Table 4). The total uncertainty of

Table 3. Densities, Virial Coefficients, and Adsorption Constants of Acetonitrile at 423.15 K Calculated by the c/d Procedure[a]

$K_r = 0.095\ 294\ 5\ cm^{-1}$ (r for $i = 20$)
$x(1)$, $\rho_r = 36.489\ mol\ m^{-3}$ ($\rho_r^* = 36.487\ mol\ m^{-3}$)
$x(2)$, $B = -1243.3\ cm^3\ mol^{-1}$ ($B^* = -1238.3\ cm^3\ mol^{-1}$)
$x(3)$, $C = 999\ 000\ cm^6\ mol^{-2}$ ($C^* = 974\ 400\ cm^6\ mol^{-2}$)
$x(4)$, $k_A = 3.63 \times 10^{-8}\ mol\ m^{-3}$
$x(5)$, $k_B = 6.10$

i	p_i/kPa	H_i/cm	ρ_i^*/(mol m^{-3})	ρ_i/(mol m^{-3})	ρ_i^{ads}/(mol m^{-3})	Z_i
1	554.4504	42.530	198.92	198.88	0.079	0.7923
2	515.4707	42.345	181.48	181.47	0.039	0.8073
3	466.7840	42.070	160.55	160.56	0.023	0.8261
4	417.5705	41.728	140.42	140.42	0.016	0.8451
5	370.9812	41.320	122.14	122.15	0.013	0.8630
6	320.3795	40.744	103.18	103.19	0.010	0.8823
7	271.7739	39.989	85.738	85.744	0.008	0.9007
8	261.9049	39.801	82.273	82.280	0.008	0.9045
9	251.7318	39.593	78.754	78.760	0.007	0.9083
10	240.3328	39.338	74.829	74.835	0.007	0.9126
11	228.7209	39.053	70.881	70.887	0.007	0.9169
12	217.9703	38.763	67.270	67.275	0.006	0.9209
13	201.4544	38.254	61.748	61.753	0.006	0.9270
14	189.5892	37.835	57.839	57.844	0.006	0.9314
15	177.7544	37.362	53.982	53.986	0.005	0.9358
16	166.8519	36.865	50.447	50.451	0.005	0.9398
17	156.0912	36.309	47.004	47.007	0.005	0.9438
18	145.1987	35.660	43.536	43.539	0.005	0.9478
19	133.2120	34.826	39.765	39.767	0.004	0.9521
20	**122.7248**	**33.961**	**36.487**	**36.489**	**0.004**	**0.9560**

[a] The asterisk means uncorrected for adsorption.

Table 4. Acetonitrile Gas Densities Corrected for Adsorption

	ρ/(mol m^{-3})				
p/kPa	403.15 K	423.15 K	433.15 K	443.15 K	463.15 K
120.	37.817	35.635		33.789	
150.	47.938	45.060		42.620	40.463
200.	65.566	61.269		57.721	54.676
250.	84.140	78.148	75.629	73.333	69.288
300.		95.753	92.397	89.488	84.327
350.		114.140	109.879	106.221	99.820
400.		133.366	128.075	123.567	115.797
450.		153.485	146.985	141.557	
500.		174.556	166.609	160.177	
550.		196.632	186.948	179.518	

the reported gas densities was estimated to be less than 0.1%, considering the uncertainties in the measurements of temperature, pressure, height of mercury in the tube, and the tube constant.

For nonpolar gases, a successful correlation of the second virial coefficient based on a three-parameter (p_c, T_c, ω) theory of the corresponding states has been proposed by Pitzer and Curl (*17*), where ω is an acentric factor. From the present vapor pressure data ω was estimated to be 0.323. It is well known that the fluids whose molecules have noncentral force fields deviate from the principle. Various extended modifications with additional parameters have been proposed. Also some other correlations that are not based on the corresponding state theory are known, for example, the method of Nothnagel et al. (*18*), which uses the chemical interpretation to explain imperfections in the vapor phase.

None of these correlational methods is good enough for predicting the second virial coefficient of non-hydrogen-bonding acetonitrile within the temperature range of the present measurements. Acetonitrile is a linear molecule and might be expected to behave like a rigid dipole, and the symbol μ stands for the dipole moment. Correlations (*19–21*) giving the best agreement with literature data were considered. In the Tsonopoulos correlation (*19*) the original values for ω and

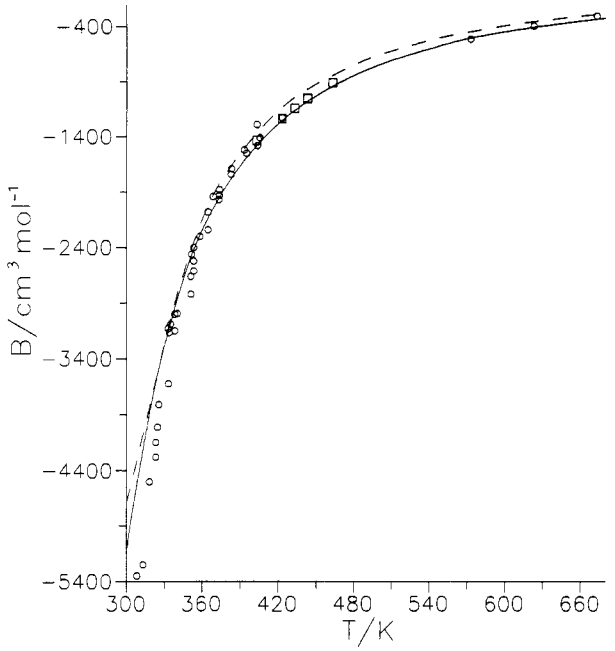

Figure 6. Experimental and predicted (by means of the Stockmayer potential function) second virial coefficients: ○, results of refs 6 and 11–16; □, this work; solid line, predicted for new force constants; dashed line, predicted for force constants reported by ref 23.

$\mu_R = (10^5\mu^2 p_c)/T_c^2$ are 0.323 and 25 371.8 D^2 kPa K^{-2}, respectively. In the O'Connell and Prausnitz correlation (*20*), the symbol ω_H stands for the acentric factor of the acetonitrile homomorph, and η for an association factor. The original values of ω_H, η, and μ for acetonitrile, viz., 0.152, 0.0, and 3.94 D, were used. The acetonitrile parameters used for the Tarakad and Danner correlation (*21*) were $\bar{R}$ = 1.821 Å for the radius of gyration and ϕ = 3.008 for the polarity factor as defined in ref 21. The correlational second virial coefficients are plotted in Figure 5. Comparison of the present second virial coefficients with those evaluated from the corresponding state correlations show deviations of 1.5–20%; the present values occur between those correlated by the equations of refs 19–21, as shown in Figure 5. The Tsonopulous correlation is the most promising for results of this work although it was derived for lower reduced temperatures, $T_R < 0.75$.

Interactions between two polar molecules may be expressed by the Stockmayer potential (*22*) as a function of σ, ϵ, and the angles which determine the relative orientation of the dipoles; σ is the collision diameter for which the potential energy is zero, and ϵ is the minimum energy of the potential. In order to calculate the second virial coefficient of a gas, the force constants have to be known and the function B^* (=$3B/(2\Pi N\sigma^3)$) for different values of T^* and t^* tabulated by Hirschfelder et al. (*23*) is used, where N is Avogadro's number, $t^* = \mu^2/(8^{1/2}\epsilon\sigma^3)$, $T^* = kT/\epsilon$, and k is Boltzmann's constant. The dashed line in Figure 6 represents the values of acetonitrile's second virial coefficient calculated for μ = 3.5 D, σ = 4.02 Å, and ϵ/k = 400 K given by Hirschfelder et al. (*23*).

Conversely, the experimental second virial coefficient data are used for determining the force constants. Different values of the dipole moment μ of the acetonitrile were found in the literature (*3*, *20*, *24*), and an average value, 3.95 D, was used. The force constants are determined from available experimental second virial coefficients including present results, and they are σ = 4.48 Å and ϵ/k = 371.4 K for t^* = 1.2. The results predicted by a new force constant are presented in Figure 6 (solid line). At the high temperature range differences between the predicted and experimental second virial coefficients agree to within the experimental error, but no configuration of $B^* = f(T^*,t^*)$ gives satisfactory results at the low temperature range.

Conclusions

In the present experimental pressure range the third virial coefficient is a substantial contribution to the total nonideality even for the pVT data close to atmospheric. An attempt was made to correct for adsorption of the acetonitrile vapor on the glass and mercury surfaces. It may be concluded that the present gas-phase results are more reliable even if the arbitrarily chosen BET model is not the right one.

The vapor pressures and saturated densities agree reasonably well, to within 0.5% with most available literature data.

Literature Cited

(1) Kreglewski, A.; Zawisza, A. C.; Wecsile, *J. Bull. Acad. Pol. Sci., Ser. Sci. Chim.* **1965**, *13* (3), 195.
(2) Aftienjew, J.; Zawisza, A. C. *J. Chem. Thermodyn.* **1977**, *9*, 153.
(3) Weast, R. C., Ed. *Handbook of Chemistry and Physics*, 62nd ed.; CRC Press Inc.: Boca Raton, FL, 1981.
(4) Hall, K. R.; Canfield, F. B. *Physica* **1967**, *33*, 481.
(5) Kratzke, H.; Muller, S. *J. Chem. Thermodyn.* **1985**, *17*, 151.
(6) Francesconi, A. Z.; Franck, E. U.; Lentz, H. *Ber. Bunsen-Ges. Phys. Chem.* **1975**, *79*, 897.
(7) Mousa, A. H. N. *J. Chem. Thermodyn.* **1981**, *13*, 201.
(8) Wagner, W.; Ewers, J.; Pentermann, W. J. *Chem. Thermodyn.* **1976**, *8*, 1049.
(9) Pentermann, W.; Wagner, W. *J. Chem. Thermodyn.* **1978**, *10*, 1161.
(10) Ter-Gazarian, G. *J. Chim. Phys. Phys.-Chim. Biol.* **1906**, *4*, 140.
(11) Kolysko, L. E.; Mozhginskaya, L. V.; Gorodinskaya, E. Ya. *Russ. J. Phys. Chem.* **1972**, *46*, 614; *Zh. Fiz. Khim.* **1972**, *46*, 1046.
(12) Zaalishvili, Sh. D.; Kolysko, L. E.; Gorodinskaya, E. Ya. *Russ. J. Phys. Chem.* **1971**, *45*, 1500; *Zh. Fiz. Khim.* **1971**, *45*, 2648.
(13) Lambert, J. D.; Staines, E. N.; Woods, S. D. *Proc. R. Soc. London* **1960**, *A200*, 262.
(14) Brown, I.; Smith, F. *Aust. J. Chem.* **1960**, *13*, 30.
(15) Prausnitz, J. M.; Carter, W. B. *AIChE J.* **1960**, *6*, 611.
(16) Lambert, J. D.; Roberts, G. A. H.; Rowlinson, J. S.; Wilkinson, V. J. *Proc. R. Soc. London* **1949**, *A196*, 113.
(17) Pitzer, K. S.; Curl, Jr., R. F. *J. Am. Chem. Soc.* **1957**, *79*, 2369.
(18) Nothnagel, K.-.; Abrams, D. S.; Prausnitz, J. M. *Ind. Eng. Chem. Process Des. Dev.* **1973**, *12*, 25.
(19) Tsonopoulos, C. *AIChE J.* **1974**, *20* (2), 263.
(20) O'Connell, J. P.; Prausnitz, J. M. *Ind. Eng. Chem. Process Des. Dev.* **1967**, *6* (2), 245.
(21) Tarakad, R. R.; Danner, R. P. *AIChE J.* **1977**, *23* (5), 685.
(22) Stockmayer, W. H. *J. Chem. Phys.* **1941**, *9*, 398, 863.
(23) Hirschfelder, J. O.; Curtiss, C. F.; Bird, R. B. *Molecular theory of gases and liquids*; John Wiley and Sons, Inc.: New York, 1954.
(24) McClellan, A. I. *Tables of experimental dipole moments*; W. H. Freeman: San Francisco, 1963.

Received for review June 1, 1993. Revised October 25, 1993. Accepted November 19, 1993.*

* Abstract published in *Advance ACS Abstracts*, February 1, 1994.